

UNIVERSITY OF TWENTE

DESALINATION ON A CHIP

BACHELOR'S THESIS

The Influences of Hydrogel Geometry on
the Desalination of Salt Water

Author:

E.G.H. Derckx

Student Number:

s1607650

Daily Supervisor:

MSc. A.M. Benneker

Responsible Supervisor:

Dr. J.A Wood

Exam Committee:

Dr. ir. D.W.F. Brilman

Prof. Dr. ir. R.G.H. Lammertink

July 28, 2017



UNIVERSITY
OF TWENTE.

Abstract

In this bachelor's thesis, the influences of geometry on ion transport on a patterned membrane stack from researchers from SFI and BIOS (MESA+ from University of Twente) are investigated. Three geometries were used with different properties regarding shape, aspect ratio and exchange area: A linear shaped ('full'), a coned shaped ('tilted') and a H-patterned ('original') shape.

The relative efficiencies of these three geometries have been investigated using amperometry. Microscopic observations were used to quantify the vortex generation (as a result of electroconvection) in each geometry. It has been found that the 'tilted' shaped membrane stack is the most efficient, using amperometry with 8 volt. Concentration profiling and vortex generation measurements have indicated that the 'original' shaped membrane stack has the highest capability to generate vortices in the system compared to the other two geometries, due to its multiple sites for vortices to nucleate from.

Specifically, it has been suggested that the vortex size affects the desalination rate as suggested by two cases that show the extremes of vortex generation (in the presence of an optimum present). Case 1: Where there is over-mixing when turbulent convection generated from the vortices limit the directional movement of ions towards the membrane, limiting the transfer rate. This is due to the vortex size being bigger than the channel width. Case 2: A lower vortex size could increase mixing properties between membranes while the depletion zone decreases.

Symbol list and abbreviations

Abbreviations

SCR	Space Charge Region
IEM	Ion Exchange Membrane
ED	Electro Dialysis
AEM	Anionic Exchange Membrane
CEM	Cationic Exchange Membrane
METC	2-(methacryloyloxy)ethyl]trimethylammonium chloride
SPAP	3-sulfo-propyl acrylate potassium salt
DMPA	2,2-dimethoxy- 2-phenylacetophenone
LIM	Polydimethylsiloxane
OLM	Limiting Region
ML	Over Limiting Region
	Mixing Layer

Symbols

D [m^2/s]	Diffusion of the ionic species
c^0 [mol/L]	Initial ion concentration
F [s*a/mol]	Faraday constant,
δ [m]	Nernst diffusion layer
T_1 []	Transport number through the electrolyte
t_1 []	Transport number through the membrane.
U [V]	Voltage
I [A]	Current
R [Ω]	Resistance
ΔP [kg/m^3]	Change of density
g [m^2/s]	Gravity acceleration
h [m]	Characteristic length
ρ [kg/m^3]	Density
ν [m^2/s]	Kinematic viscosity

Contents

1	Introduction	5
2	Theory	7
2.1	Membrane Characteristics	7
2.2	Regimes	8
2.3	Diffusion Boundary Layer	11
2.4	Mechanisms in the over limiting regime (OLM)	11
2.4.1	Gravitational Force	12
2.4.2	Water Splitting	13
2.4.3	Ion Properties	14
2.4.4	Electroconvection and Vortices	14
2.5	Geometry Influences	15
2.6	Current Efficiency	16
3	Experimental Procedure	18
3.1	Membrane Geometries and Specifications	18
3.2	Procedures	19
4	Results and Discussion	20
4.1	Impedance measurements	20
4.2	IV sweeps	22
4.3	Amperometry	26
4.4	Vortex Generation measurements	29
4.5	Current Efficiency Results	35
5	Conclusion	36
6	Recommendation for future research	37
7	Appendices	40

1 Introduction

Desalination of brine water is key in providing the world with sufficient drinking water. Fresh water sources are declining due to climate change and human interference with nature. Creating a new economically feasible way to desalinate water will effectively increase the global freshwater resin significantly. At the moment, water treatment facilities are immense and needs a lot of engineering capital and energy. New methods to desalinate brine water must be found to supply the world with enough freshwater [1].

One approach to solve this issue is to use Ion-Exchange Membranes (IEMs) with electrodialysis (ED) to desalinate water. Electrodialysis is a way to filter ions from a solution using an external electric field. This electric field in combination with an IEM can remove ions from its solution based on electro-osmosis and charge-selective transport through membranes. Key factors in this desalination process are the membranes ability to transport ions, which is related to the geometry of the ionic exchange membrane. However, before this method can be expanded upon on applications, there must be more fundamental knowledge gained about ion transport in such IEMs systems.

There already are some numerical simulations of ionic movement (based on Poisson-Nernst-Planck and Navier Stokes descriptions) (by Dydek and Bazant [2] and researchers from within SFI) near an IEM. However, these models and theories lack experimental data to confirm its validity. There is still much to be learned about the movement of ions in a IEM, and the way to gain this knowledge is to be found using experimental work. [2]

A microfluidic electrodialysis stack for investigation of ion transport was developed by researchers from SFI and BIOS (MESA+, University of Twente), in which alternating anion- and cation exchange hydrogels are patterned in a PDMS chip. No in-depth experiments were done on the ion transport and the influence of membrane geometry with this platform. The system can be seen in Figure 1. As of now, the device has only been tested using one simple geometry and there are no known experimental papers testing this system (or other systems) with different geometries. The device in question can be altered regarding its geometry in various shapes by altering the shape of the capillary barrier. Therefore, the option of discovering a more feasible design regarding its geometry is possible. As the fundamental fluid dynamics in the membrane are rather difficult to grasp and lacking in experimental data, finding relations with the geometries in these kind of systems will progress the understanding of the movement of ions in a IEM. [2]

The device in question works as as shown in Figure 1: When an external electric field (E) is applied over the membrane, Na^+ ions will travel towards the cathode side and Cl^- ion will travel towards the anode side. This is due to drift of ions in the applied electric field (electro convection). The systems desalination property is present due to the alternating Anion Exchange Membrane (AEM, green in the figure) and the Cation Exchange Membrane (CEM, red in the figure). Due to these barriers, the cation ions are stuck near their countering membrane type, resulting in accumulation of ions near the membrane. This will result in alternating concentrated flows (red) and depleted flows (blue).

It is known that the surface area of the membrane greatly influences the depletion efficiency, especially the ratio between channel sizes and length (aspect ratio) [4]. A similar effect is seen on the shape of the membrane and its ability to (direct) bend the direction of the electric field lines within the membrane that is generated by the electrodes. The bent electric field will influence the

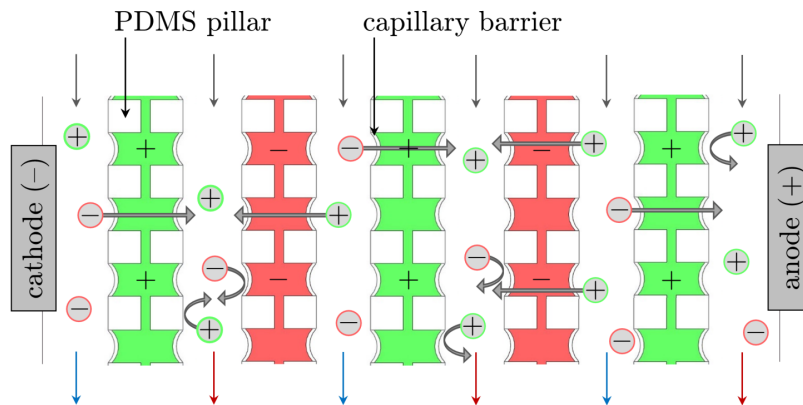


Figure 1: *Schematic overview of the membrane stack from MESA+[3]. Alternating anion and cation exchange hydrogels are positioned in a PDMS chip. If an electric field is applied over the stack, ions are selectively transported, resulting in alternating concentrated (red arrows) and desalinated (blue arrows) flows.*

flow direction of the ions. This electric field is the main contributor to vortices that appear due to electroconvection that will greatly influence mixing capabilities and thus the concentration near the surface. Which results in a higher driving force at the membrane surface, and thus a higher desalination rate.

In this academic assignment, the aforementioned desalination method is tested using the membrane stacks developed by researchers from SFI and Bios (MESA+, University of Twente). The purpose of this assignment is to expand upon the proof of concept of Gumuscu et al. [3], with an emphasis on the fluid dynamics of ions regarding the geometry of the membrane stacks.

2 Theory

In this section, membrane characteristics of the system under investigation are discussed. The mechanisms of ion transfer are introduced, and the influence of the geometry on the IEM capabilities are discussed.

2.1 Membrane Characteristics

The system consists of alternating AEM's and CEM's. The AEM's and CEM's are polymers that have the ability to transfer charge specific ions depending on the sign of the ions. This ability stems from the membrane charged surfaces. The CEM is negatively charged and the AEM is positively charged.

The AEM is made of *[2-(methacryloyloxy)ethyl]trimethylammonium chloride* (METC) and the CEM is made from *3-sulfopropyl acrylate potassium salt* (SPAP). These compounds were photo polymerized with acrylamide and *(N,N-bis(2-hydroxyethyl)ethylenedi-amine)*. The monomers were cross-linked by *2,2-dimethoxy-2-phenylacetophenone* (DMPA) by randomly associating. The polymer chains were polymerized in the illuminated region. For further reading, see the article: *Desalination by electro dialysis Using a Stack of Patterned Ion-Selective Hydrogels on a microfluidic Device* from Gumuscu et al. [3].

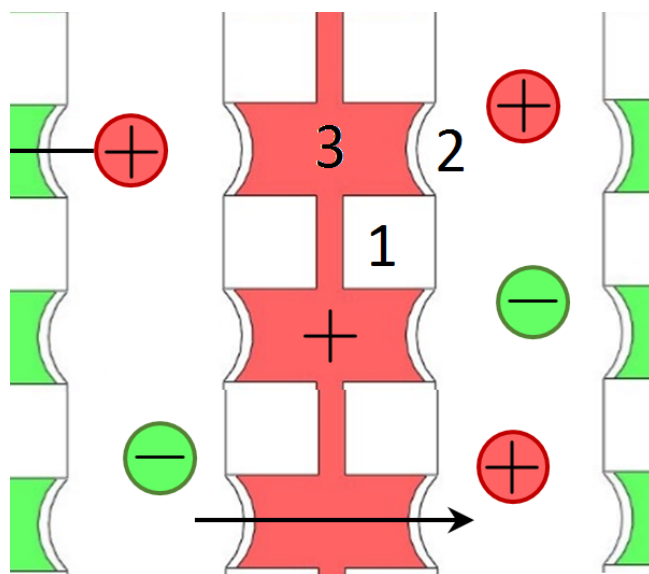


Figure 2: The membrane stack is constructed with use of the PDMS stamps (and its pillars). The system can be divided in eleven channels; five channels to pour the membrane in and six channels where the brine water is directed through. The membrane channels are filled with the hydrogels and are sealed. Legend: 1) Is a PDMS pillar created from the stamp. 2) Capillary barrier created to ensure the hydrogels position. 3) is the SPAP/METC (AEM, CEM).

In general, hydrogels are very hydrophilic and swell upon contact with water. The surface of this hydrogel membrane has a very specific surface charge. It is very important that the surface

charge is kept constant, as mass transfer rates will decline due to loss of surface charge, lowering the overall driving force of the system. The surface charge of the membranes integrated in the system is independent from pH values ranging from 2 to 12. This pH in-dependency is key to this system as water splitting, might occur during electro dialysis, can affect the pH in the solution. See section subsection 2.4.2 which explains water splitting. [3, 5]

However, the hydrophilic property of the membrane also results in a not fully selective membrane. As the swelling increases, the capacity of the membrane to uphold their charged surfaces decreases, as the water will make contact with the charged surface (due to the increased surface area from swelling), lowering the specific charge of the membrane and thus its capability to selectively transfer ions. The hydrophilicity changes the permeability of the membrane for ions to transfer through the membrane. [6]

	AEM (METC)	CEM (SPAP)
Swelling in deionized water (%)	460 + 10	450 + 10
Ion exchange capacity (mmol $\frac{g}{dry}$)	1.96 + 0.45	0.64 + 0.09
Resistivity (Ohm cm) (single meas.)	310	470
Charge density (mol L H_2O^{-1})	0.43 + 0.10	0.14 + 0.02
Permselectivity (%)	29	26

Table 1: *Physical properties of the AEM (METC) and the CEM (SPAP) as found by Gumuscu et al. [3]. One can note the ion exchange capacity difference of the membranes. The AEM has a higher ionic exchange capacity. The charge density of the AEM is also higher, which probably results in a higher activity near the AEM.*

2.2 Regimes

In electro dialysis, ions migrate due to the influence of an external electric field. This effect is called electro-osmosis and is the basis of electro dialysis. The current is a measure of the amount of ions moving through the membrane. Depending on the potential of the electric field, different (mass transfer) phenomena occur within the membrane stack, leading to different kinds of ion transfer near the membrane surface. These phenomena are categorized in three regimes. The three regimes are the Ohmic regime, the limiting regime (LIM) and the over limiting regime (OLM). This phenomena have been observed in various papers [3, 7, 2]. It is possible to experimentally observe these regimes using an IV-sweep (current vs applied potential) which is shown in *Figure 3*.

The reason why these regimes occur is due to the ability of the membrane stack to create different concentration gradients in the membrane-solution interface when these are put under the influence of external driving forces like an electric field. This phenomenon is called concentration polarization. Concentration polarization is the phenomena that charges accumulate near the membrane surface. This is because of the co-and counter ion transport rates which differ from each other. This accumulation near the surface membrane constructs the boundary layer, contributing mass transfer resistance in the membrane stack. These different concentration gradients occur due to the membrane's property to transfer some species in the solution more readily than others as the system, consists of two different membranes, with each different specifications (this can be seen in

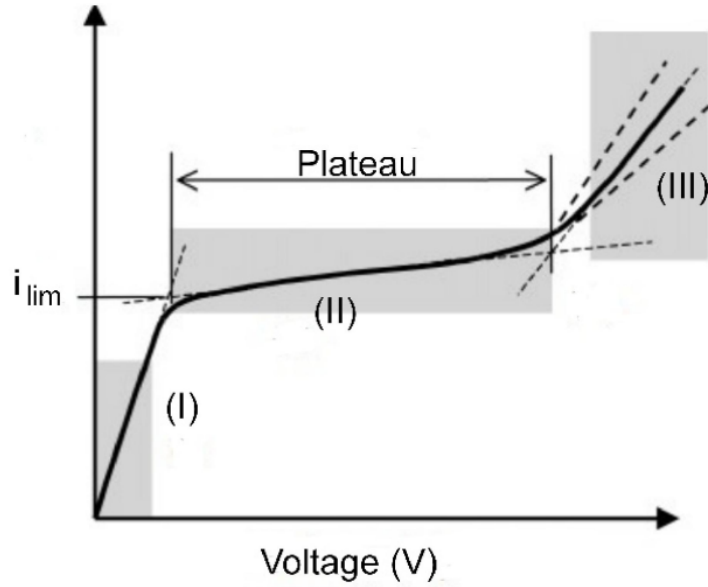


Figure 3: *IV Sweep shown from an IEM cell. The current is shown against the potential difference over the membrane stack. The three regions can be seen due to its difference in gradients (which indicates different transport mechanisms in the system).*[8]

the experimental section in Table 1). This concentration polarization is responsible for the systems non linearity across the three regimes. [9]

In the Ohmic regime, which occurs at relatively low potentials, the membrane stack experiences an Ohmic resistance. This states that the resistance in the system is linear in the form of Ohm's law $U = IR$. The main mechanisms in this regime which drive ion transport are ion drift and ion diffusivity in the solution. [7]

In the limiting regime, mass transfer rates will not (or barely) increase even though voltage is increased unlike in the Ohmic regime. In the limiting region, diffusion (and migration) through the membrane is relatively slower than the transport through the solution. This results in a low ion concentration near the membrane surface. A constant increase in conductivity is observed even when the potential is increased. Water splitting and electro-osmosis (of the second kind) start to occur but are still limited and do not influence the system in a significant way. This explains the small but noticeable gradient in the limiting region, as can be in Figure 3. [9].

The limiting current can be seen by observation of IV sweeps (experimental work) or through the well-known theoretical equation Equation 1 [10].

$$i_{lim} = \frac{Dc^0F}{\delta(T_1 - t_1)} \quad (1)$$

Where D is the diffusion of the ionic species, c^0 is the initial ion concentration, F is the Faraday constant, δ is the Nernst diffusion layer T_1 is the transport number through the electrolyte and t_1 is

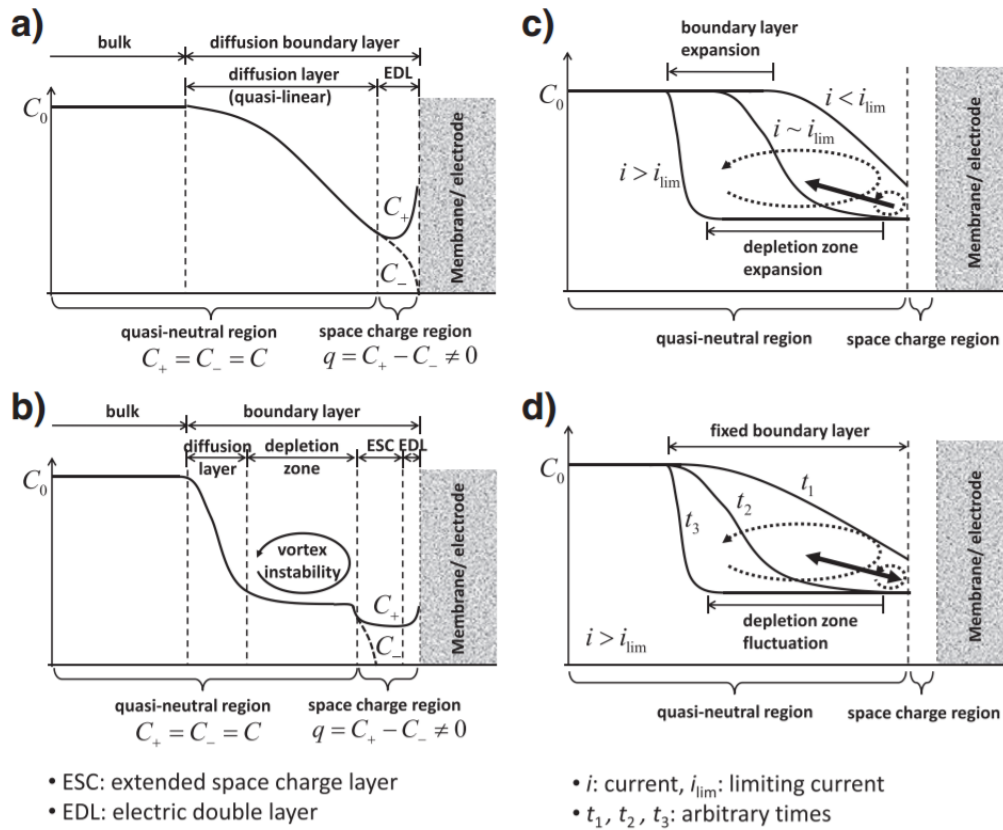


Figure 4: a) Model of conventional concentration polarization based on the electric double layer and space charge region, b) Structure of boundary layer caused by ion concentration polarization found with experimental work, c) change of modified resistance regimes on model presented in subfigure a), d) Over-limiting regime test taken on different arbitrary times t using experimental work. [11]

the transport number through the membrane.

In the over limiting regime, the resistance from the boundary layer formed from ion concentration polarization is altered. The high voltage from the external electric field acts on the local charge non-neutrality and the space charge regions (SCR), which is a layer of counter ions near the charged surface of the membrane. In the over limiting regime, electro convective forces start to play the main role. Vortices appear due to ionic movement following the generated external field. This electroconvective vortex will result in a degree of mixing with the bulk concentration allowing the concentration near the membrane to increase. This also influences the space charge region in electric double layer, as the degree of mixing increases due to the convective forces introduced in the system. These vortices could greatly influence the desalination rate of the membrane stack by increasing the overall driving force through the membrane.

Figure 4 shows the concentration profiles and the influences of the regimes and their effect on the depletion zone. At a) the electric double layer can be seen and the concentration difference trough

the zones. At b) an over limiting current is introduced, showing the change of co-ion concentration near the membrane surface. In particular, at c)/d) in the figure, the over limiting current expands the depletion zone, introducing more ions from the bulk concentration towards the surface concentration indicating that in the over limiting region, the driving force increases.

2.3 Diffusion Boundary Layer

The Diffusion Boundary Layer (DBL) is a layer in which the ions must travel through to reach the exchange area. This layer contributes to the overall mass transfer resistance in the membrane stack. Nikonenko et al. [6] has shown that the DBL can be distinguished into two regions: The quasi-electroneutral region and the space charge region (SCR). The space charge region contains the electric double layer of the membrane and an extended region in which the local anion and cation concentration are not equal. This effect is the constructor of the electric double layer.

Figure 5 shows the concentration profile near the an ionic exchange membrane in these three regions. The depletion zones increase in width as the current increases. This has also been seen in Figure 4. At first, concentration gradients follow are only affected by the current due to ion drift (from the external electric field). Then it enters the space charge region, where co- and counter ions move at different rates towards the membrane area. Then, when close towards the exchange area, concentrations of the co-ions increase due to space charges being present at the surface. These co-ions on the left of the membrane, must respond to the counter-ion on the right of the membrane, as this will drive the ion movement through the membrane. [6]

The Electric Double Layer (EDL) is the layer where the anion concentration and cation concentration near the membrane are not in charge equilibrium. i.e. the solution is not neutral charged. The electric double layer is the major part of the space charge region and contributes to the mass transfer resistance in the membrane stack. [12]

The width of the space charge region is dependent on a few factors: The charge and mobility of the ionic species in the electrolyte, the surface charge on the membrane, the strength of the external electric field and if applied, the convective flow in the system. In general the space charge region increases as a higher external field is applied, as the counter-ions are more attracted towards its respective electrode. This results (in principal) in a wider space charge region. A convective flow of the electrolyte will take away these loosely bounded ions near the surface which decreases the width of the space charge region, lowering the mass transfer resistance experienced in the membrane stack. [7]

As the space charge region has a net charge (either positive or negative, depending on the sign of the membrane's charged surface), the electric field will act on this region, causing fluid movement. The local direction of the electric field lines influences the direction of movement of the fluid, which influences mixing properties in the membrane stack.

2.4 Mechanisms in the over limiting regime (OLM)

In this section, the mechanisms in the over limiting region will be discussed. The over limiting region is very interesting for this system, as in this region the generation of vortices are actively present

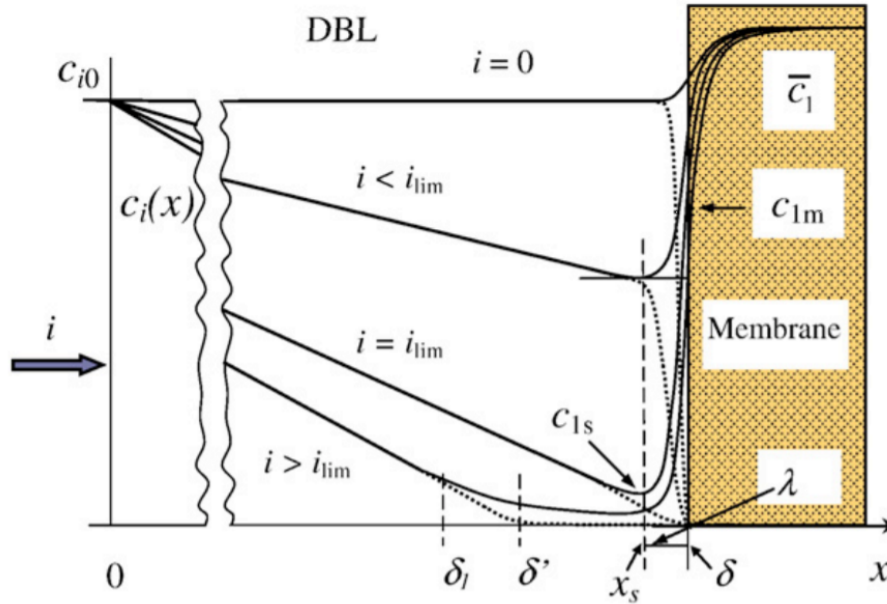


Figure 5: Scheme of an ED cell boundary layer near a AEM in the different regimes. $0 < x \leq \delta_1$ is the electro neutral layer, $\delta_1 < x \leq \delta$ shows the space charge region. The δ' shows the effective thickness of the electric double layer. The layer between x_s and δ is the quasi equilibrium boundary layer. The dotted lines show the counter ion and the full line shows the co-ion.[6]

compared to the tiny and almost non-existent vortices that are found in the limiting region.

2.4.1 Gravitational Force

When a electric field is generated across the IEM, density gradients develop near the membrane surface due to local concentration differences. This results in natural convection created by the density difference, this movement follows Archimedes' law [13]. Gravitational forces (and thermal convection) can be described using mass transfer numbers, such as the Grashof number (which correlates buoyancy forces and viscous forces) and the Prandtl number (which correlates thermal diffusivity versus momentum transport). The product of these two numbers result in the Rayleigh number ($Ra = Gr * Pr$). The Rayleigh number states the buoyancy driven force in the system, which is generally known as natural (or free) convection.

Gravitational forces (and thermal convection) can be neglected if Rayleigh number is below a certain critical value. This critical value is 1708 as stated in the article from [14].

$$Pr = \frac{v_k i n}{\alpha} \quad (2)$$

$$Gr = \frac{\Delta P * g * h^3}{\rho v_k^2} \quad (3)$$

Where ΔP is the change of density, g is the gravity acceleration, h the characteristic length, ρ the density and ν the kinematic viscosity.

Following calculations it has shown that gravitational forces can be mainly neglected in IEMs which use diluted concentrations. These diluted concentrations are in a low order of magnitude, which results in almost zero influence of the gravitational forces at hand. Also Nikonenko et al. [6] stated that in dilute systems, that gravitational convection is insignificant and should not be taken into account.

2.4.2 Water Splitting

Water splitting is the chemical reaction of water converting into its ion counterparts following reaction Equation 4. Water splitting can occur due to a high electric potential acted upon the solution. This water splitting reaction produces ions which can also travel through the membrane, limiting the mass transfer opportunities of the projected salt ions, which is key for desalination. This effect is known as the exaltation effect. These water splitting reaction mainly occurs in the layer near the membrane surface, where electric field lines are concentrated. [5]



Where the kinetics of the forward reaction is $2 \cdot 10^{-5} \frac{1}{s}$ and the reverse reaction $1.5 \cdot 10^{14} \frac{cm^3}{mol \cdot s}$ [13]

However, there are some reports that the reaction kinetics shown above are not correct. As in non-dilute systems it has been found that the rate of water splitting occurs at much higher rates. Nikonenko et al. [6] has suggested another mechanism where there is neutral base B which originates from the membrane, is involved in the reaction. However, this has not been proven yet and will not be taken into account.

The exaltation effect is critical for the system's desalination efficiency. The ionic mobility of the created hydrogen and hydroxide ions are about five times the mobility of the targeted salt. This indicates that these ions are more likely to travel through the membrane. Which results in an overall lower desalination rate in the membrane stack.

	H^+	OH^-	K^+	Cl^-
Mobility $10^{-8} m^2 s^{-1} V^{-1}$	36.23	20.64	7.62	7.92

Table 2: Ionic mobility per ion [15]

Local pH changes can indicate the occurrence of water splitting and the formation of additional ions. To check if water splitting occurs at all, a pH measurement could be done to check the degree of water splitting in the system. However, previous work done with ionic exchange membranes [11] indicates that in the concentration range where the system is operated during experiments, no significant pH changes of the fluid were observed. This was experimentally confirmed using pH measurements with the membrane stacks. This leads to the conclusion that water splitting is probably not present in this system.

2.4.3 Ion Properties

In traditional systems, the Peclet number (Pe) is used to describe the mass transport in the system regarding diffusion versus convection. However, it was found that the Stokes' radii of the ions can describe the mass transfer rate as well. The Stokes radius of chloride is lower than the radius of the sodium as can be seen in table Table 3. This may result in higher electroconvective movement of the ionic species and thus higher vortex generation at the CEM side of the membrane. [11]

If the Stokes radius is smaller, the diffusion coefficient must be higher, as they are inversely proportionate. This can also be related to Peclet's number (Pe), where an higher diffusion coefficient results in a lower Peclet number which indicates that convective forces are less present for the respective ionic species.[12]

	Stokes Radius $\mu\text{ m}$	Diffusion coefficient m^2/s
Sodium ion	0.183	$1.334 * 10^{-9}$
Chloride ion	0.120	$2.032 * 10^{-9}$

Table 3: *Stokes Radii and Diffusion coefficient of the main ions*

This indicates that chloride ions are more likely to transfer in the system, which results in higher activity near the CEM side of the membrane stack.[16]

2.4.4 Electroconvection and Vortices

Electroconvection (also called the second form of electro-osmosis) is the key mechanism in this system. As an electric field is applied to the system, ions in the solution move towards their charged electrode counterpart, resulting in a flow of ions. Electroconvection is the main reason that vortices appear. The movement of the ions collide with the non-slip surface of the membrane and with external electric field lines, this will result in ion motion. This movement is due to these effects in a circular motion near the membrane. Figure 6 shows the motions near the membrane pores. These vortices can influence the diffusion boundary layer by expanding the depletion zone, creating a 'mixing layer', in which surface concentrations are heavily mixed with the bulk concentration resulting in a higher concentration at the membrane's surface. As for the space charge region in the diffusion boundary layer, it will decrease due to the mixing properties of these vortices resulting in lower mass transfer resistance through the membrane stack.

Vortices are in general suppressed when shear flow is applied through the system. The generation of a vortex is not instant and depends on the potential of the electric field. Due to this dependency on the strength of the electric field, vortices only appear consistently in the over limiting regime. In general the size of the vortex increases as the electric potential increases [17].

These vortices do not stay stationary in the system, as they tend to advance over the length of the membrane. However, these vortices do not migrate but rather shift along the membrane, resulting in larger vortices at the end of the membrane. This can be seen in Figure 7.

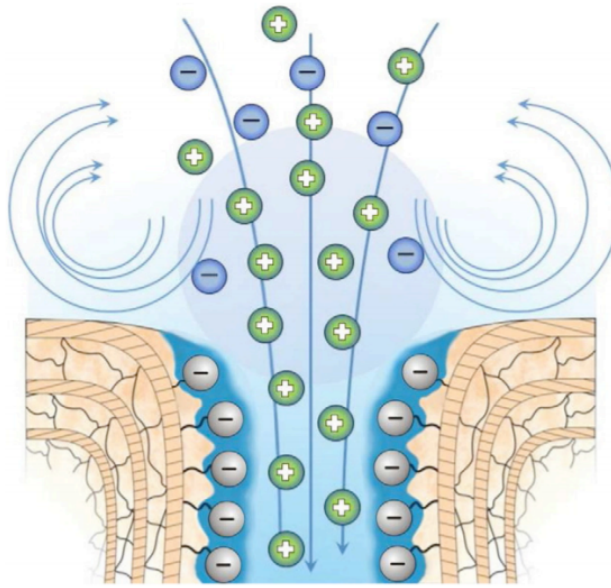


Figure 6: A schematic illustration showing the motion of ions near the pores of the membrane. [6]

The system in general is operated in the laminar region, but due to velocity and momentum created by the vortices, the system rather evolves into a locally turbulent regime. The Rayleigh number changes dynamically over time, altering the influence of gravitational forces (and thermal forces) in the system. However, due to the dilute solutions used in the system, this effect is negligible. [14]

2.5 Geometry Influences

Membrane geometry is a key factor in the efficiency of the membrane stack, as different shapes and dimensions of the membrane can alter the efficiency greatly. If the membrane has a local non-conduction region, ionic transport is more condensed, resulting in different mass transfer rate through the pores of the membrane. However, the lower exchange area also results in less 'spots' for ion to be exchanged through the membrane.

In structured membranes the vortices have preferred sites to generate which are the ridges of exchange area of the membrane (CEM and AEM). This is due to the velocity of the electrolyte that is directed toward the corner of the structure, with inflow from above the gap and outflow above the extrusion. These sites are responsible for the relation between the vortex size and structure, as are the exchange area and the aspect ratio of the membrane stack. However, it is key for the mixing property that the vortices are stable, as a higher degree of vortices will result in such turbulent vortices that the velocity of the ions/electrolyte to the membrane interface will suffer.[18]

When considering the morphology of the membranes, de Valença [18] has investigated the influence of membrane pillars in the channel of the system, while observing the velocity lines in the membrane. It has been shown that vortices on a flat surface start to move on random location along the length of the membrane, while at a structured membrane the vortices are pinned at the structure

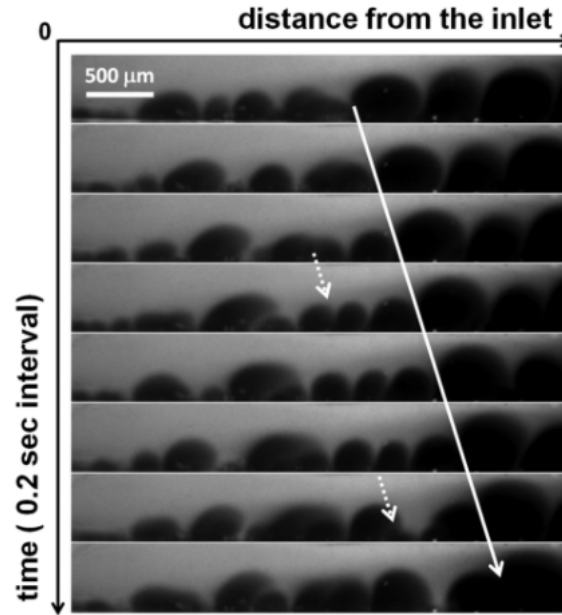


Figure 7: Vortex shifts along the length of the membrane [17].

edges.

2.6 Current Efficiency

Current efficiency is a term which gives a quantitative answer for the efficiency of the system and can be seen in equation Equation 5. The current efficiency indicates the amount of energy (generated from the external field on a constant current) that is usefully used in the desalination process. [11]

$$CE = \frac{zF\phi_v(C_{Concentrated} - C_{Desalted})}{2NI} \quad (5)$$

Where z is the charge of the ion, F is the Faraday constant, ϕ_v is the volume metric flow, N the amount of unit cells in the ED cell, C the concentration of the salt and I the current applied to the system.

Another method to indicate the efficiency of the cell is to compare the amount of ions that enters the system versus the amount of ions transferred based on the measured current while doing amperometry. Using Equation 6 and Equation 7 the efficiency can be calculated in equation Equation 8.

$$Ions_{transferred} = \frac{Na_a}{F} \int_0^t I(t)dt \quad (6)$$

Where N_a is the Avogadro constant, $I(t)$ the Current-time relation found experimentally and F the Faraday constant.

$$Ions_{supplied} = 2 * \phi_v * C_0 * N_a * t \quad (7)$$

C_0 is the initial (monovalent) salt concentration. The factor 2 is introduced due to the salt dissolving into two ions.

$$\eta_{ions} = \frac{Ions_{transferred}}{Ions_{supplied}} \quad (8)$$

3 Experimental Procedure

In this chapter the experimental procedures are explained. Sodium Chloride (NaCl) is used as model salt due to its simplicity and inexpensiveness. This thesis does not use any divalent salt (or other monovalent salts). An image of the set-up can be seen in Figure 8. Additional information of the equipment used in the set-up can be found in the Appendix.

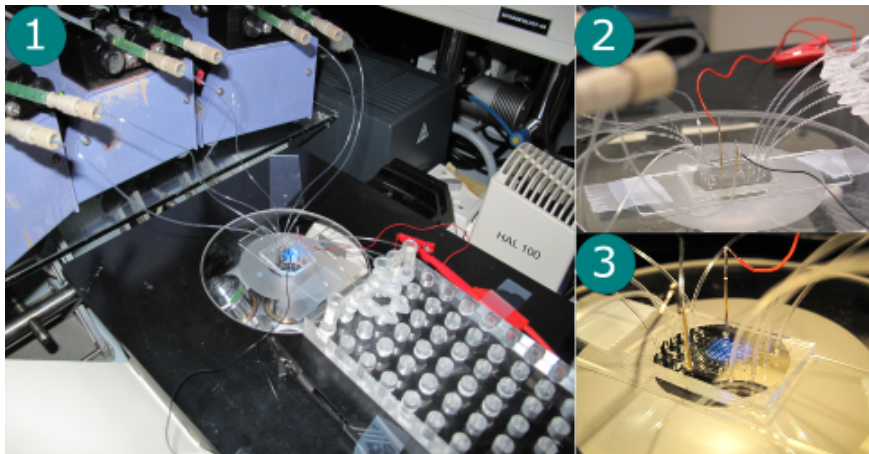


Figure 8: *Experimental set-up: (1) Image of the set-up, the membrane is put under a Inverted microscope and is connected to three micro pumps. The electrodes are connected to a potentiostat. (2) Close up of the connections on the membrane. (3) Another close-up.*

3.1 Membrane Geometries and Specifications

During the experimental phase, experiments were done on three different membrane stacks. The 'original' shape as was used in the proof by concept paper from Gumuscu et al. [3], a 'full' shape and a 'tilted' Shape. These membrane stacks can be seen in Figure 9.



Figure 9: *The three membrane stacks that are used. Left: Type 1, also called the 'original' shape. Middle: Type 6, also called the 'full' shape and Right: Type 7 also called The 'tilted' shape.*

The geometries at hand were chosen as these showed the most potential for gaining knowledge about ion-movement in the membrane stack. The 'original' shape is used as a calibration geometry, to check the proof by concept work from Gumuscu et al. [3]. This will be the reference geometry. The 'full' shape was chosen for its linearity and high exchange area. With this geometry the generation of vortices are to be expected on the low end, as there are no favorable sites like in the 'tilted' and

'original' membrane stacks. The 'tilted' membrane stack is expected to have relative high vortex generation near the small membrane area ridges and a low vortex generation near the wide area ridges. It is to be expected that these vortices of random shapes and sizes will create a lot of chaos in the system allowing to study its effects. This will randomize the mixing layer's concentration drastically. The dimensions of the three membrane stacks can be found in Table 4.

	Original 1 [μm]	Tilted 6 [μm]	Full 7 [μm]
Channel Y	690	690	1000
Channel Y at Hydrogel	867	955	-
Hydrogel Y	1550	1465	1000
Hydrogel X	690	295-1725	16100
Pillar X	690	690	-
Aspect Ratio	0.0363 []	0.0328 []	0.0392 []
Exchange Area	0.0047 [m^2]	0.0055 [m^2]	0.0253 [m^2]

Table 4: *Dimensions of the three membrane stacks used, Channel Y is the height of the channel, hydrogel X is the width of the hydrogel and hydrogel Y is the length of the hydrogel. Pillar X is the distance between two membranes. Supporting information about the calculations the Exchange Area can be found in the Appendix.*

3.2 Procedures

The measurement are done using a Autolab program that is connected to a potentiostat. Images were made using a high speed camera and a tracer solution (See Appendix).

An IV Sweep is used to find the three regimes in the system. The potentiostat applies a DC voltage on the electrodes, which creates an electric field over the membrane. The potentiostat measures the current at that electric potential and moves to the next voltage. The step size is 0.05 volt/s and the range of these voltage ranges from 0 until 9.95 volt.

Ampero/potentiometry uses a DC signal and measures the current/voltage in a set time range. This procedure is used to acquire samples from the membrane stack and investigating the current vs time relation.

FRA (Frequency Response Analyzer) measurements are measurements which measures the impedance of the membrane stack (Z). Impedance is the resistance for an AC circuit likewise to DC circuits. DC circuits cannot be used when measuring the resistance of these solutions, as the one-way current that the DC signal generates, result in migration of the ions. This migration greatly influences the resistance of the solution due to the already low concentration used during experiments. As such, FRA measurements will be done as this mitigates this problem. The impedance of the solution will be measured and a calibration curve of can be made to find the concentration of the desalinated and brine water channels.

4 Results and Discussion

4.1 Impedance measurements

Impedance (Z) can be measured using a Frequency Response Analyzer (FRA). Impedance is a complex number[19], which means that the impedance can be split in a real and imaginary part. In general, the impedance can be quantified using the following equation.

$$Z = \frac{E_t}{I_t} = Z_0 \frac{\sin(\omega t)}{\sin(\omega t + \phi)} \quad (9)$$

Where ϕ is the phase shift, Z_0 is the amplitude of the signal, ω the frequency of the signal and Z the impedance.

This can equation can be rewritten using Euler's formula to split it into a complex number:

$$Z(\omega) = Z_0(\cos\phi + j\sin\phi) \quad (10)$$

In these impedance measurements, $-Z''$ and Z' can be found. When plotted against each other, a Nyquist Plot can be constructed. This plot consists of a real part (X-axis) and an imaginary part (Y-axis). What is interesting for our system is the 'real part', or in other words, where the plotted line intersects with the X-Axis. The first intersection of these plot shows the Ohmic resistance (R_Ω) of the solution, the second intersection shows the total resistance of the system. Using the first intersection and the trajectory of the plot, a calibration curve could be constructed.

As seen in the Figure 10, the calibration curve that was constructed did not show any valid results. If the results are fitted the curve results in a negative Ohmic resistance, which is impossible to have in reality. The error calculated from the measurements was also too great to quantify a calibration curve. We did not measure a monotonic increase in resistance with reduction in concentration, which is also an indication that these measurements are not to be used.

One explanation of this phenomena of negative resistance is due to the induction of the electrode. Even though that the electrodes are protected and magnetic inductance should not interfere, it would be possible that this occurred in the slightest, which still would be enough given the non-conducting property of the electrode (very low ion concentration).

Due to this, another measure must be taken to quantify the efficiency of the membrane stacks. So Equation 8 will be used instead to define ion efficiency of the membrane stacks.

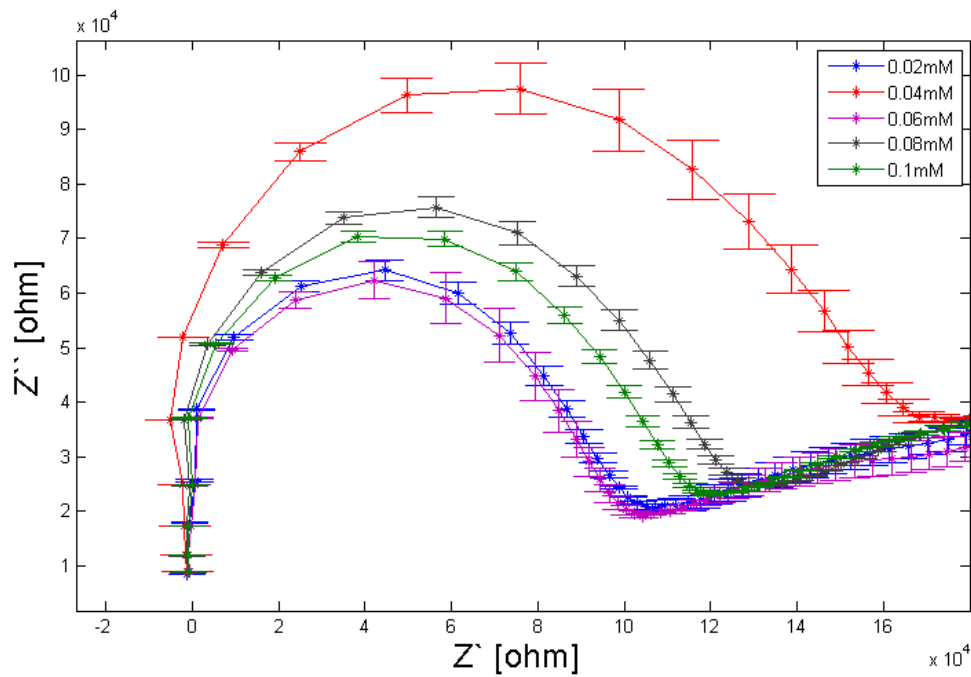


Figure 10: Z' vs $-Z''$ of the FRA measurements, experiments were done in quintuple. The dotted lines represent the 95 percent confidence bounds. As can be seen in this figure, the confidence bounds of concentrations overlap significantly. Due to this overlapping and high error values, using these kind of curves are not usable to make quantitative conclusions from the data at hand. Measurements were done from 1Hz to 1MHz.

4.2 IV sweeps

IV sweeps show the electric response of the system, and are an indication for the different transport regimes in the system. These IV sweeps can be used to analyze the ion transport in the membrane stack. The gradient of the IV sweeps states the conductivity of the membrane stack. This is however, only true in the Ohmic regime. After the Ohmic regime, one can see the current fluctuate. This fluctuation is due to overall mechanisms in the system when entering the over-limiting regime (and the limiting regime).

However, the gradient can still be used to investigate the resistance in the over-limiting region to give a degree of the resistance that is experienced in the membrane stack.

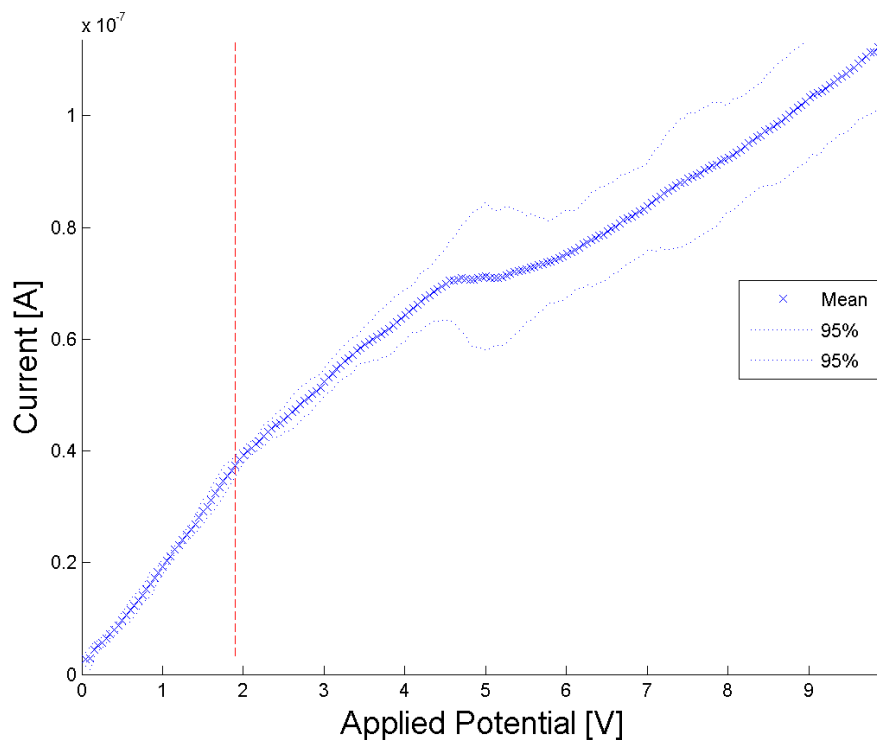


Figure 11: *IV sweep of the 'original' shape, the dotted lines represent the standard deviation. The red line represent the limiting region transition point based on the change of gradient of the curve, indicating that the limiting current has been met. This can also be related to the increase of standard deviation as this introduces the vortices which mainly appear in the over limiting regime. The flow rate in this particular IV-Sweep was $5 \mu\text{l}/\text{min}$. Experiments were done in triplicate. The step size is $0.05 \text{ Volt}/\text{sec}$.*

The standard deviation can be used as a measure of chaos in the system introduced by the vortices. The standard deviation will be used to quantify the vortex generation and general mixing of the membrane stack. Due to the chaos begin present in this system it is hard to find reproducible

measurements.

It can be seen in Figure 11 that the standard deviation increases as voltage increases, specifically, the standard deviation increases when the limiting regime (which is more a limiting point) is traversed. This increase in standard deviation appears due to vortices in the system, however, not only does the voltage affect vortex generation. The time spent on the applied voltage is also a big factor. Vortices do not appear instantly and need time to generate along the microchannel. In general the standard deviation will increase as the vortex has more time to increase in size resulting in an increase of mixing properties.

What is suppressing these vortices is the flow that is perpendicular to the electric field direction. This flow greatly suppresses the vortex as the generation rate is relatively low and thus the small vortices get swept by the shear flow. This shear flow also refreshes the salt concentration in the channel. As can be seen in Figure 12 and Figure 13 the conductivity decreases as the flow increases. This is likely due to the shear flow suppressing the vortices that increases the mixing layer and thus lowering the overall transport of ions through the hydrogels.

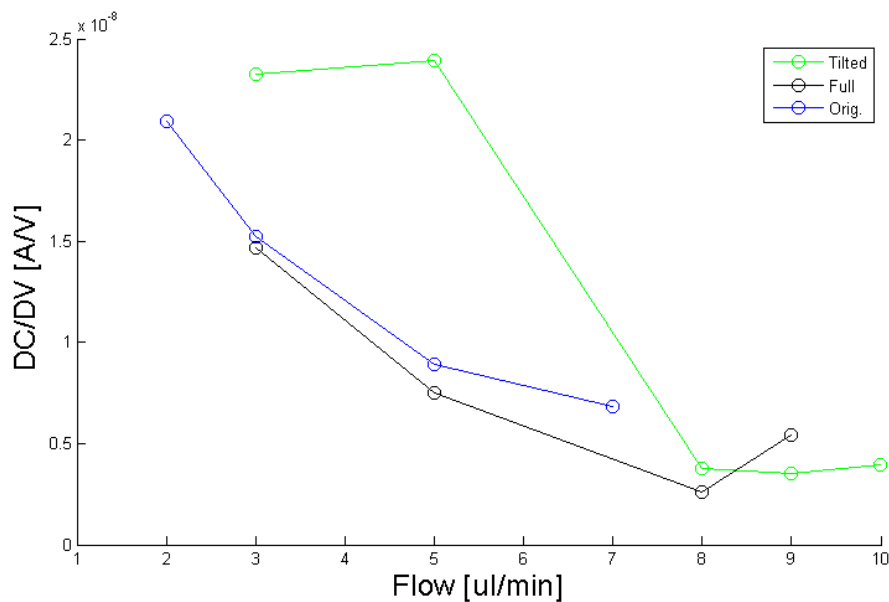


Figure 12: Gradients from IV curves in the OLM. The conductance ($\frac{\delta I}{\delta V}$) is shown for the three geometries used during experiments.

If the conductance of the membrane is taken into account, the geometry's influence can be noticed as can be seen in Figure 12. A remarkable point is that the 'full' geometry has the highest exchange area but is in the same order of magnitude of the other two shapes. This is probably due to the amount of sites where vortices can be created. Due to these factors, the current 'evens' out with the other geometries, but when normalized against the exchange area in Figure 13, one can see its in-effectiveness of desalination per square meter.

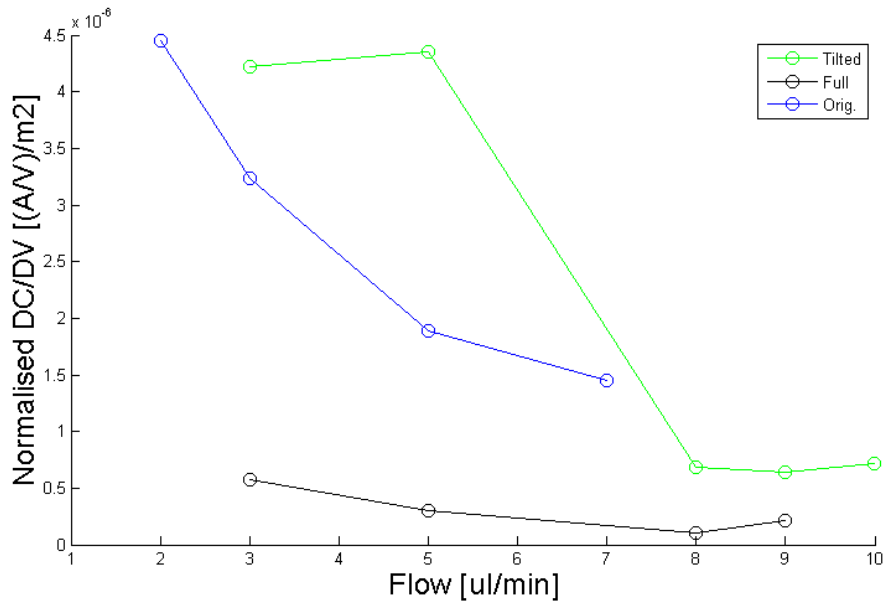


Figure 13: Same as Figure 12 however, the values are normalized against the exchange areas of the respective geometries.

Comparing the 'tilted' and the 'original' geometries which both have about equal exchange area do differ from each other in terms of conductance. A probable cause is the likely hood of vortices in the system. To quantify these vortex generations, the standard deviation of the current is compared of each geometry in Figure 14. As seen in the figure, the 'tilted' shape deviation is lower through the IV-sweep than the 'original' one, which could indicate that the 'original' shape is higher capable of creating vortices in the system than the 'tilted' shape.

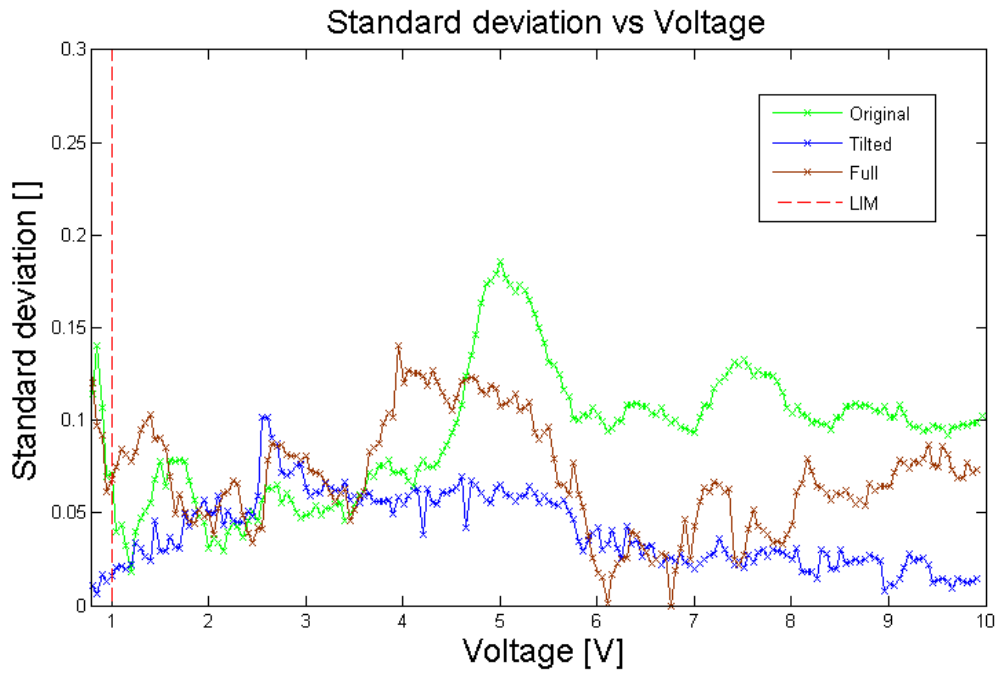


Figure 14: *Standard deviation vs voltage at a flow condition of 5 $\mu\text{l}/\text{min}$ of the three main geometries. As can be seen in the figure, the standard deviation of the 'tilted' shape is rather limited when compared to the 'original' and 'full' shape. In correlation with Figure 15 the error range of the tilted shape is rather limited.*

To further investigate this vortex generation within each membrane, amperometry is used at long time intervals to allow the vortex to generate in the membrane stack. This will be done at a constant voltage. These measurements will give insight to the maximum vortex generation and the generation cycles the vortex takes.

4.3 Amperometry

Amperometry is done to quantify the efficiencies of the membrane stacks. The amperometry measurements are always done at an electric field potential of 8 Volt. 8 Volt is used as it is sure that vortices appear and that the over-limiting region is reached. The measurements are done for 180 seconds.

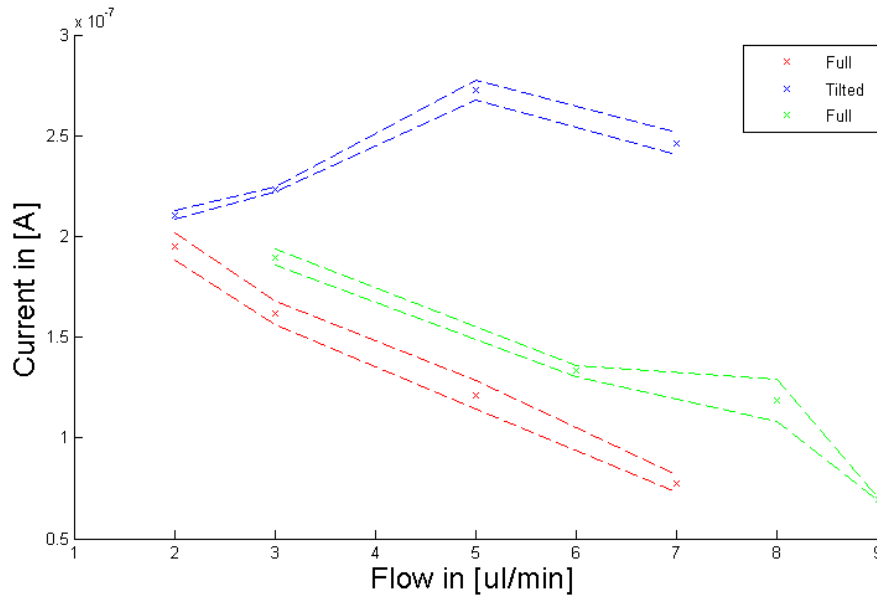


Figure 15: *Amperometry results per geometry using different shear flows.*

Figure 15 shows the absolute values of the current measured versus the applied flow. It is clear that the 'tilted' shape has the highest current at every shear flow. These graphs suggest that the 'tilted' shape is the best geometry to use as it has the highest current values. When comparing with Figure 16 it still shows that the 'tilted' shape is on top even regarding the normalization with the exchange area.

A noteworthy feat from the 'Full' shape, is that the absolute current is close to the 'tilted' and 'original' shape as was found in the conductance measurements. However, when normalized against its high exchange area of the membrane, the current per square meter decreases a lot relative to the other geometries. This could indicate that even though the membrane per square meter is not very effective, due to effective use of the space given which allows for a lot of exchange area per membrane stack as the current is still rather in the same order of magnitude.

However, the mixing capabilities and vortex generation for the 'original' and 'tilted' ions are still not clear yet. The difference for the conductance could be due to different mixing capabilities. It is suggested that that are two cases which could explain this current difference regarding electro-convection.

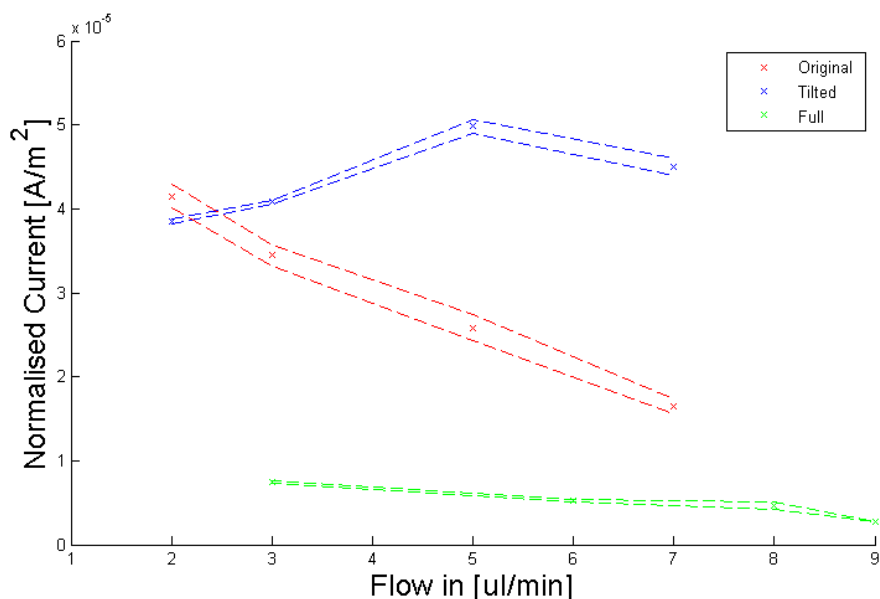


Figure 16: Values from Figure 15 normalized against the exchange area of the respective geometry.

Case 1: Interfering vortices

There is a possibility that vortices from the AEM and CEM can interfere with each other if the electric potential applied is strong enough to create vortices that are bigger than the radius of the channel. Due to this, the vortices consistent of cations and anions are able to move all over the membrane, mitigating the positive effect of the vortex. Due to this chaos, it could be possible that the ions in the solutions move at such velocities that it is impossible to efficiently pass through the membrane.

Case 2: Incomplete mixing

Another possibility is that the vortices from the AEM and CEM are smaller than the radius of the channel. Resulting in a brine stream of the bulk concentration in the middle of the channel. The mixing due to vortices is severely cut but the overall concentration near the surface would decrease.

The two cases would lead to an optimum of vortex size versus the measured current. These two cases could be seen as the boundary conditions of this maximum, or in general, the extremes of the membrane stacks capabilities.

To investigate these cases, a model is used to suggest mixing properties of these cases, as for experimental work, time was a constraint and could not be identified in a proper manner using microscopy. A model provided from within SFI can simulate electric field lines in the channel, granting the possibility to view the mixing trends in the membrane with use of the electric field lines distribution in the membrane stack, granting insight on the directional movement of the ions.

Electric field line distribution

Using Figure 17 it is possible to derive mixing qualities in the different membrane stacks. It is clear that the electric field lines in the 'original' membrane stack do not interact with other membranes in the same channel. The membranes in essence work independent from each other with each membrane part having a different bulk concentration. This indicates rather low mixing qualities in between the membrane part, when compared against the 'tilted' membrane stack. The 'tilted' membrane stack's electric field lines are more distributed along different membranes, this could result in a better mixing between each membrane, resulting in a higher degree of mixing. The electric field along the microchannel induces electro-osmotic flow, which suggests easier vortex formation. T

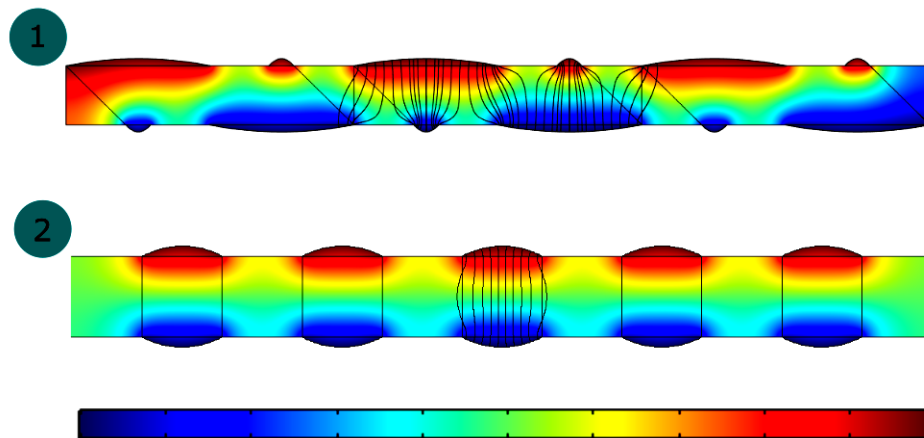


Figure 17: *Electric field bending and potential distribution in the 1) 'tilted' shape membrane stack and the 2) 'original' shape membrane stack. A flow condition of $3 \mu\text{l}/\text{min}$ and an maximum potential difference of 0.5V . legend: the red color is the maximum of electric potential at the field and blue is the least.*

To further investigate these field lines and the mixing qualities amperometry with a microscope will be used to investigate the vortices generation and movement throughout the measurement. The visualization is done using a negatively charged fluorescent dye (*Alexa 488 Cadaverine*).

4.4 Vortex Generation measurements

Original

In Figure 18 the progression of the ion depletion zone under a no-flow condition is shown as a function of time. At 8 seconds, a layer on the CEM side is formed, this indicates the pigmented dye travelling with the ions through the membrane and being depleted from the membrane interface. At 22.5 seconds, vortices (indicated by local high intensity of the dye) start to appear from the ridges of membrane area, similar what was found by de Valença [18]. Also note the white illuminated region near the AEM, which indicate ion depletion as well. At 60 seconds, a new phenomena occurs, there is a depleted cation concentration zone near the rims of the membrane, it is not known at this moment how these depleted zones are created. At 165 seconds and on, vortices are done evolving and stabilize. In this picture however, it is possible to see the depleted ion zone near the PDMS pillar of the membrane in regards to the bulk of the feed. What is remarkable here is that the exchange region is covering more than half of the channel height.

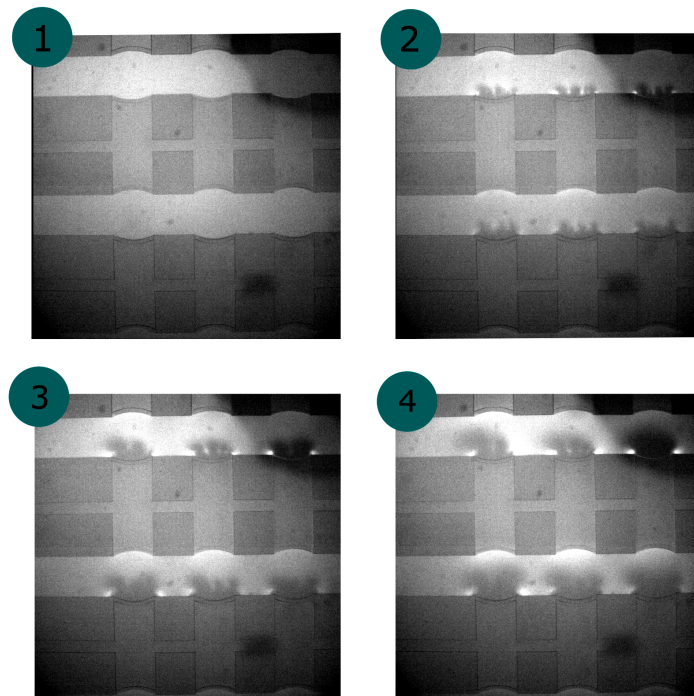


Figure 18: *Vortex snapshots at different times under a no-flow condition and a potential applied of 8 volt. Channels 3 and 4 are shown 1) At 8 Seconds. 2) At 22.5 seconds. 3) At 60 seconds 4) At 165 seconds.*

Vortex generation in a no flow condition has been simulated using numerical simulations. In Figure 19 the velocity lines at the 'original' symmetrical membrane are shown. The model has a few limitations, as it does not account for the different Stokes ion radii, so the vortices created will be completely symmetrical, which in reality is not the case. The velocity decreases due to the depletion

of ions in the channel, as this is a no-flow conditioned model with boundary conditions of total depletion. What is interesting is the aftermath the vortex, as it seems to mix the solution in the part near the outlet of the membrane. However this effect is probably due to the model, considering the outlet to be a non permeable layer and thus creating velocity lines as if it was approaching a corner. This needs to be verified experimentally.

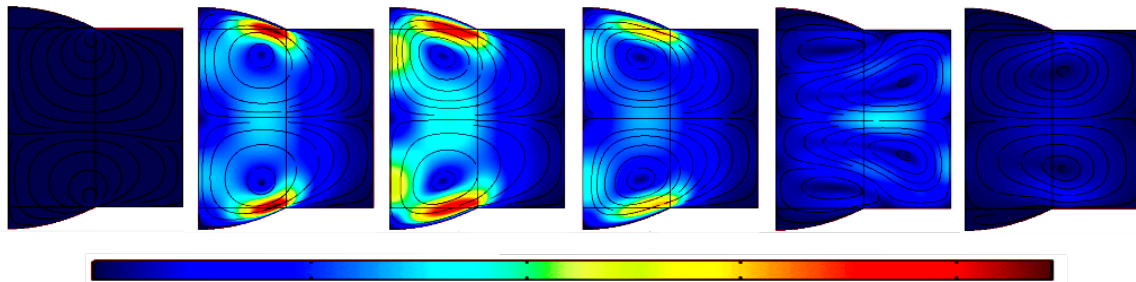


Figure 19: Vortex generation at a no flow condition. Times (from left to right) normalized against (L^2/D) : $e-6$, $3e-4$, $7e-4$, 0.001 , 0.007 and 0.1 seconds at 0.5 volt

For comparison with a flow condition of $2 \mu\text{l}/\text{min}$, Figure 20 is used. This figure is a close up from channel number three at the inlet of the membrane. It can be clearly be seen that the vortex generation over time with flow is greatly suppressed, as also the growth of the depletion zone is suppressed. At 200 seconds one can see a transport region being created at the membrane exchange area. At 400 seconds this area increases. At 520 seconds and on, the area does not increase, indicating that vortices are not possible to develop further in these kind of flow situations. Resulting that applications with these kind of micro separators to be very difficult if operating on any volume metric flows. Also note that the depletion zone at the outer rims of the membranes are not present anymore.

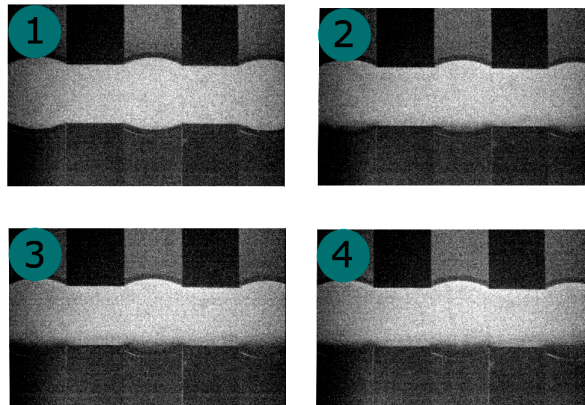


Figure 20: Vortex snapshots at different times T for $2 \mu\text{l}/\text{min}$ and a potential applied of 8 volt at times: $1) = 0$, $2 = 200$ sec, $3 = 400$ sec. $4 = 520$ seconds.

This vortex generation pattern can also be seen in the model over time. The vortex size is related

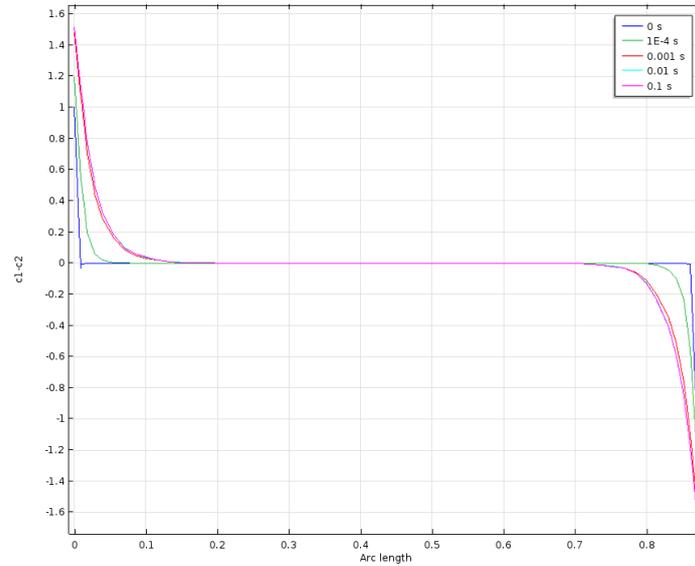


Figure 21: *Concentration difference (for a ion species) versus channel per time step width plotted from simulation results. The length is normalized against the channel width of the membrane stack ('original'). Time is normalized against the diffusion time scale (L^2/D).*

to the size of the depletion zone. As the vortex increases, the depletion zone increases as well over time (while suppressed due to the applied flow.). In Figure 21 it can be seen that the concentration over the width of the channel fluctuates from the bulk concentration as time progresses. This is the same what was seen during observations in the depletion (exchange) zones (Figure 20). The plot shift along the width of the channel per time step, this indicates the depletion zone increase over time.

'Full' Shape

The 'Full' shape ability to create and sustain vortices are severely limited if compared to the original shape. As can be seen from a close up in Figure 22, the depletion region is not to be found along the surface of the membrane. There is some contrast found between the AEM surface and the CEM surfaces, this is however still very limited. However, it has been found that at different places along the channel and at all channels vortices appeared randomly and disappeared randomly. This randomness can be explained due to the lack of favorable sites for the vortices to nucleate. For a convective term applied to the system the vortex generation is close to zero and thus disappear almost instantly.

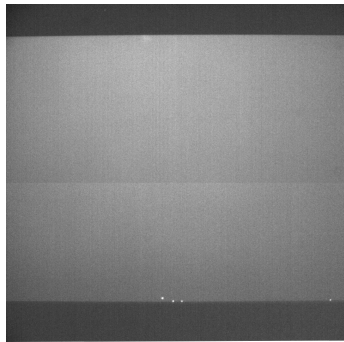


Figure 22: 'Full' shape snapshot At 300 seconds at a flow of $3 \mu\text{l}/\text{min}$ with an electric potential of 8 volt. Ion depletion zones are greatly suppressed because of the cross flow applied through the microchannels.

'Tilted' Shape

The 'tilted' shape geometry has very concentrated and small exchange regions at the small hydrogel parts, but thin and wide exchange regions near the wide hydrogel parts. These vortices do not extend (at the same voltage) over more than half of the channel. This could indicate that mixing properties were different for the ions in the bulk as for the surface concentration. It seems that this shape is less capable of creating violent vortices than the 'original' shape. But it must be stated that the channel height y at the hydrogel for the tilted shape is bigger than its original counterpart, allowing more space for the vortices to develop. The difference in channel height is about $100 \mu m$ but could make the difference in these kind of microfluidic systems.

These differences in vortex dimensions regarding the height of the channel y suggest that vortices, when vortices are smaller than the radius of the channel height are able to mix in such a way that ions can move more easily through the system. As for the geometry, comparing the 'tilted' and 'original' shapes, the 'tilted' shape has an ability to sustain smaller vortices at the exchange area than the 'original' shape. This can be linked to the electric field line distribution found in the model.

This also suggest that the 'original' shape, is in a sense, a more efficient geometry than the 'tilted' shape for creating vortices. As the 'original' shape is more capable of creating vortices, the applied potential field could be dimmed down to acquire similar currents as has been seen with these measurements at 8 volt, but was not done due to time constraints

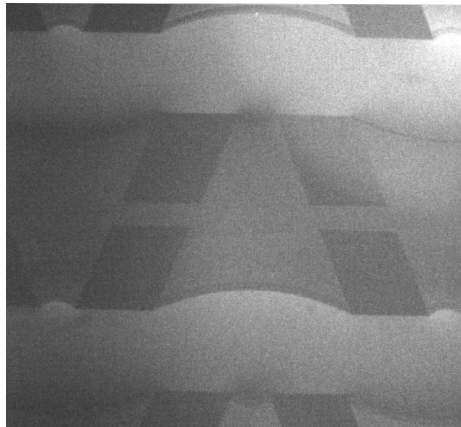


Figure 23: *tilted shape snapshot at 300 seconds, at a flow condition of $0 \mu l/min$ and an electric potential applied at 8 volt.*

As for comparing the 'tilted' shape no flow condition with the same geometry under flow, when a flow is introduced to this system, the already rather small vortices that are visible in the no flow condition get suppressed. Studying figures Figure 24 one can see that the transfer region is still visible but very limited.

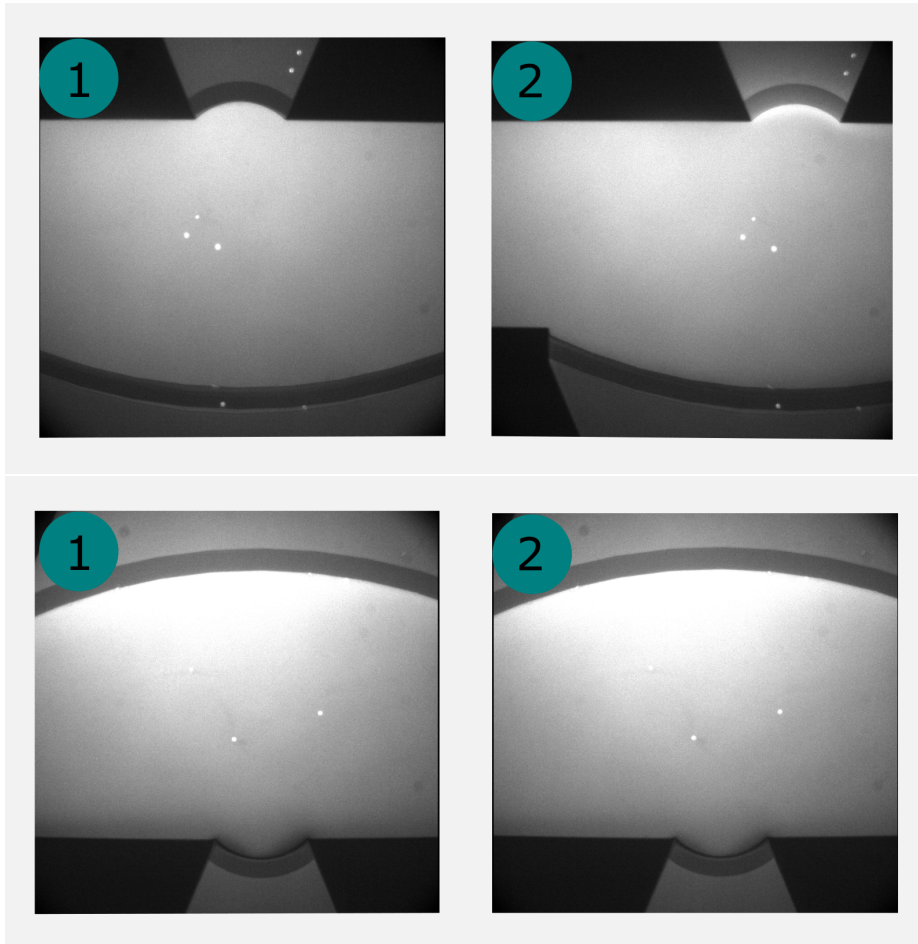


Figure 24: Vortex tilted at 3 at inverted position and the normal position

4.5 Current Efficiency Results

Finally, the efficiency of the membrane stacks are investigated, using the amperometry measurements, the total current can be found over time. Results are shown in Figure 25. Using equation Equation 8 the efficiency can be found. The results are similar of what was found in the conductance vs flow diagrams. The tilted shape is still the most efficient at this potentials. What is remarkable is that the efficiency follows a inverse proportionate relationship with the flow applied. Which has also be found in Figure 12, as for the absolute values, those can be seen in Table 5.

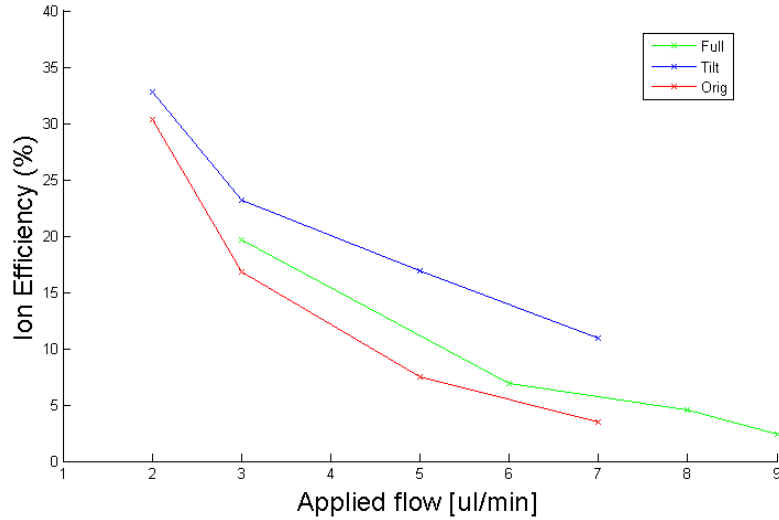


Figure 25: Efficiency (Using absolute current)(%) calculated with equation Equation 8 for different applied flows.

	2 $\mu\text{l}/\text{min}$	3 $\mu\text{l}/\text{min}$	5 $\mu\text{l}/\text{min}$	7 $\mu\text{l}/\text{min}$
original (%)	30.31	16.78	7.543	3.433
tilted (%)	32.75	23.17	16.96	10.94
Full (%)	-	19.67	11.15	5.77

Table 5: Table of efficiency's per flow setting.

5 Conclusion

In this report, we have investigated the influence of hydrogel geometry on the desalination of salt water, using I-V sweeps and amperometry to find the relative efficiencies of the three geometries studied. Microscopic observations were used to quantify the formation of depletion zones and vortex generation (as a result of electroconvection) in each geometry.

We were unable to quantify the cell efficiency of the three different membrane stacks due to the non-valid and non-linear calibration curve from the FRA measurements, which relied on the conductivity and the ion efficiency to analyze the three geometries. However, we have been able to do indicative electrical characterization of the different geometries. In this analysis it has been found that the 'tilted' shaped membrane stack is the most efficient using amperometry with 8 volt followed by the 'original' and 'full'. Vortex generation measurements have found that the 'original' shaped membrane stack has the highest capability to generate vortices in the system compared to the other two geometries, with the 'tilted' shape not falling far behind. The 'full' shaped membrane stack is the least able to do this, which can be linked towards the efficiency of these membrane stacks. This has been linked to the membrane's geometry ability to bend electric field lines in the system (Figure 17).

A negative relation has found between the applied fluid flow rate and the conductivity of the system using I-V Sweeps (Figure 12). Another relation was found, showing that the flow had negative influence on the ion efficiency of all the membrane stacks (Figure 25).

Ion zone depletion and vortex generation measurements have indicated that the vortices created in these measurements affect the desalination rate of the different membrane stacks. Specifically, it has been suggested that the vortex size affects the desalination and that a optimum is present as function of the potential applied to the membrane stack, as there are probably two cases of vortex mixing in the system.

Case 1: Where there is over-mixing when turbulent convection generated from the vortices limit the directional movement of ions towards the membrane, limiting the transfer rate. This is due to the vortex size being bigger than the channel width.

As for Case 2: A lower vortex size could increase mixing properties within the depletion zone (and the aftermath between membranes), however to test these cases, vortex visualization techniques must be used at different flows and electric potentials to quantify this effect. See the recommendations for more details on these hypotheses.

6 Recommendation for future research

Research Recommendations

Knowledge about mixing in the system at the moment is rather limited. The mixing between membranes due to vortices must be investigated to assess the potential of the vortices. Specifically, when mixing is quantified in the system another form of electro dialysis could be used. The system could use pulsed field electro dialysis, in which the electric field is switched off quickly and turned on again. The depletion zones and vortices will generate and die out again between the pulses, creating a turbulent mixing region in the system. This will decrease the space charge region mass transfer limitations, as will the concentrations mix over the channel. With the knowledge of the vortex generation and geometries of the membrane stack, this method could be realized.

Previous results have suggested that the 'original' shape is more capable of creating vortices than the other shapes. However, the scaling laws of these vortices regarding its different geometries are not found yet, only a general description [17]. The influence of exchange area, electric field line distribution and potential difference on the generation of vortices must be found. This can be found using pixel by pixel analysis of images found by the microscope. A requirement for this relation to be found is a accurate microscope which can make high resolution images.

Experimental Recommendations

Connecting in- and outlet tubing at the moment is done with manually inserting tubes in the membrane, which has a high risk of leakage near the tubing intersections, creating bubbles in the membrane, which interrupts measurements. This greatly influences the reproducibility of the system. It is recommended to use an expandable tube, which expands at the inlet of the membrane to prevent leaking. As of now, this micro-chip is very fragile when it comes to tubing, limiting the flow applied to be very low ($\approx 10 \mu\text{l}/\text{min}$).

With up-scaling, the system will face a lot more issues. When up-scaling, it will be necessary to increase the concentration used in the system to use for its targeted applications. Higher concentrations can lead to a higher degree of gravitational forces in the system, turning the system into a more turbulent system with convection going all over the membrane. As for the increase of the electric potential to desalinate further, water splitting will occur more often, increasing the effect of the exaltation effect, leading to lower desalination efficiencies.

Acknowledgements

I like to thank research group Soft Matter, Fluidics and Interfaces (SFI) for a great time and the overall help I got from everyone. As for my supervisors Msc. A.M. Benneker and Dr. J. A. Wood, who guided me through my research.

References

- [1] Matti Kummu, Philip J Ward, Hans de Moel, and Olli Varis. Is physical water scarcity a new phenomenon? global assessment of water shortage over the last two millennia. *IOP*, 5(3), 2010. doi: 10.1088/1748-9326/5/3/034006.
- [2] E. Victoria Dydek and Martin Z. Bazant. Nonlinear dynamics of ion concentration polarization in porous media: The leaky membrane model. *Alche*, 59(9):3539–3553, 2013. doi: 10.1002/aic.14200.
- [3] Burcu Gumuscu, A. Sander Haas, Anne M. Benneker, Mark A. Hempenius, Alvert van der Berg, Rob G. H. Lammertink, and Jan C. T. Eijkel. Deslination by electrodyalisis using a stack of patterned ion selective hydrogels on a microfluidic device. *Advanced Functional Materials*, pages 1–9, 2016. doi: 10.1002/adfm.201603234.
- [4] Scott M. Davidson, Matthias Wessling, and Ali Mani. On the dynamical regimes of pattern-accelerated electroconvection. *Scientific Reports*, 2016. doi: 10.1038/srep22505.
- [5] Yoshinobu Tanaka. 7 - water dissociation. In Yoshinobu Tanaka, editor, *Ion Exchange Membranes (Second Edition)*, pages 123 – 159. Elsevier, Amsterdam, second edition edition, 2015. ISBN 978-0-444-63319-4. doi: <https://doi.org/10.1016/B978-0-444-63319-4.00007-9>. URL <http://www.sciencedirect.com/science/article/pii/B9780444633194000079>.
- [6] Victor V. Nikonenko, Natalia D. Pismenskaya, Elena I. Belove, Philippe Sstat, Patrice Huguet, Gérald Pourcelly, and Christian Larchet. Intensive current transfer in membrane systems: Modeling, mechanisms and application in electrodialysis. *Elsevier*, 160:101–123, 2010. doi: 10.1016/j.cis.2010.08.001.
- [7] Yoshinobu Tanaka. 17 - bipolar membrane electrodialysis. In Yoshinobu Tanaka, editor, *Ion Exchange Membranes (Second Edition)*, pages 369 – 392. Elsevier, Amsterdam, second edition edition, 2015. ISBN 978-0-444-63319-4. doi: <https://doi.org/10.1016/B978-0-444-63319-4.00017-1>. URL <http://www.sciencedirect.com/science/article/pii/B9780444633194000171>.
- [8] T. Scarazzato, D. C. Buzzi, A. M. Bernarder, J. A. S. Tenorio, and D. C. R. Espinosa. Voltage curves for treating effluent containing hedp: Determination of the limiting current. *SciELO*, 2015.
- [9] Yoshinobu Tanaka. 6 - concentration polarization. In Yoshinobu Tanaka, editor, *Ion Exchange Membranes (Second Edition)*, pages 101 – 121. Elsevier, Amsterdam, second edition edition, 2015. ISBN 978-0-444-63319-4. doi: <https://doi.org/10.1016/B978-0-444-63319-4.00006-7>. URL <http://www.sciencedirect.com/science/article/pii/B9780444633194000067>.
- [10] Peers. *Discussion of the Faraday Society*, 21, 1956.
- [11] Rhokyun Kwak, Guofeng Guan, Weng Kung Peng, and Jongyoon Han. Microscale eletrodialysis: Concentration profiling and vortex visualization. *Elsevier*, 308:138–146, 2013. doi: 10.1016/j.desal.2012.07.017.
- [12] G. T. Barnes and I. R. Gentle. *Interfacial Science: an introduction*. Oxford University Press, second edition edition, 2011. ISBN 978-0-19-957118-5.

- [13] Zdenek Slouka, Satyajyoti Senapatie, Yu Yan, and Hsueh-Chia Chang. Charge inversion, water splitting, and vortex suppression due to dna sorption on ion-selective membranes and their ion-current signatures. *Laghuir*, 29:8275–8283, 2013. doi: 10.1021/la4007179.
- [14] V. I. Zabolotskii, V. V. Nikonenko, M. Kh. Urtenov, K. A. Lebedev, and V. V. Bugakov. Electroconvection in systems with heterogeneous ion-exchange membranes. *Russian Journal of Electrochemistry*, 48(7):692–703, 2012. ISSN 1608-3342. doi: 10.1134/S102319351206016X. URL <http://dx.doi.org/10.1134/S102319351206016X>.
- [15] Nils G. Walter. Chemical properties. URL <http://www.umich.edu/~chem260/winter00/lecnotes/lecture35.pdf>.
- [16] MIT OpenCourseWare. Ion concentration polarization. 2014.
- [17] Rhokyun Kwak, Van Sang Pham, Kian Meng Lim, and Jongyoon Han. Shear flow of an electrically charged fluid by ion concentration polarization: Scaling laws for electroconvective vortices. 2013. doi: 10.1103/PhysRevLett.110.114501.
- [18] Joeri C. de Valença. Overlimiting current properties at ion exchange membranes. 2017. doi: 10.3990/1.9789036543149.
- [19] *Basics of Electrochemical Impedance Spectroscopy*.

7 Appendices

Equipment used during experiments

Descriptions of equipment used during the experiments:

-The syringes (ID: 4.69mm) are inserted in the pumps after begin filled with 0.1 NaCl solution.

- Pumps that were used were Harvard Apparatus Pico plus pumps which could operate at a minimum of 3 microliters per minute. The tubing that was used was Flexible tubing with an inner diameter of 0.010 inch and an outer diameter of 0.030 inch.

-Nova 2.0 and Hokawo were used to process the signals from the microscope and potentiostat. During microscope measurements, light were off to improve the contrast of the fluorescent dye which was Alexa 488 Cadaverine.

Membrane preparation

Dustless paper towers are used to absorb any excessive water from the membrane, as the membranes always rest in water to prevent them from drying out. After all excessive water has been absorbed, the tubing is connected in the 6 inlets and the 6 outlets. After the tubing is done, the electrodes are connected on the chip. The electrodes are secured into position using candle wax.

Membrane Area calculations

The calculations of the membrane exchange area are based on a few assumptions. The membrane covers to the maximum top and bottom of the channel height. The Channel is a perfect tube and thus, half of the circumference is taken as the radial dimension of the area. Multiplying this number by the width of the membrane results in the Area of 1 particular membrane. Multiplying every particular membrane with the total amount of membranes result in the total area of the membrane stack.